Cell

Histone H1 Depletion in Mammals Alters Global Chromatin Structure but Causes Specific Changes in Gene Regulation

Yuhong Fan,[1] Tatiana Nikitina,[2] Jie Zhao,[1] Tomara J. Fleury,[3] Riddhi Bhattacharyya,[1] Eric E. Bouhassira,[1] Arnold Stein,[3] Christopher L. Woodcock,[2] and Arthur I. Skoultchi[1,*]
[1] Department of Cell Biology, Albert Einstein College of Medicine, Bronx, NY 10461, USA
[2] Department of Biology, University of Massachusetts, Amherst, MA 01003, USA
[3] Department of Biological Sciences, Purdue University, West Lafayette, IN 47907, USA
*Contact: skoultch@aecom.yu.edu
DOI 10.1016/j.cell.2005.10.028

SUMMARY

Linker histone H1 plays an important role in chromatin folding in vitro. To study the role of H1 in vivo, mouse embryonic stem cells null for three H1 genes were derived and were found to have 50% of the normal level of H1. H1 depletion caused dramatic chromatin structure changes, including decreased global nucleosome spacing, reduced local chromatin compaction, and decreases in certain core histone modifications. Surprisingly, however, microarray analysis revealed that expression of only a small number of genes is affected. Many of the affected genes are imprinted or are on the X chromosome and are therefore normally regulated by DNA methylation. Although global DNA methylation is not changed, methylation of specific CpGs within the regulatory regions of some of the H1 regulated genes is reduced. These results indicate that linker histones can participate in epigenetic regulation of gene expression by contributing to the maintenance or establishment of specific DNA methylation patterns.

INTRODUCTION

The DNA of all eukaryotes is packaged into chromatin through its association with histone proteins (van Holde, 1989; Wolffe, 1998). There are five major classes of histones: the core histones H2A, H2B, H3, and H4 that constitute the protein components of nucleosome core particles and the linker histone H1. In higher eukaryotes, the stoichiometry of nucleosome core particles and the linker histone is usually considered to be about equimolar, suggesting that H1 plays an important structural and/or functional role in chromatin. In vitro studies indicate that linker histones can influence chromatin structure and gene regulation (Thomas, 1999; Vignali and Workman, 1998). H1 binds to nucleosome core particles near the entry/exit sites of linker DNA (van Holde, 1989) and facilitates the folding of chromatin into a ~30 nm fiber (Bednar et al., 1998; Thoma et al., 1979). The presence of bound histone H1 also has a strong inhibitory effect in vitro on nucleosome mobility (Pennings et al., 1994) and transcription (Laybourn and Kadonaga, 1991; Shimamura et al., 1989). Although linker histones are not required for assembly of nuclei under certain experimental conditions in vitro (Dasso et al., 1994), they do appear to be important for the structural and functional integrity of mitotic chromosomes (Maresca et al., 2005). However, most of the functions attributed to H1 have not been tested in vivo. In addition, it is now clear that H1 is not essential for growth and cell division in several unicellular eukaryotes (Patterton et al., 1998; Ramon et al., 2000; Shen et al., 1995; Ushinsky et al., 1997). Thus, the precise in vivo roles of linker histones remain elusive (Thomas, 1999; Vignali and Workman, 1998).

To determine the in vivo functions of H1 in higher eukaryotes, an experimental system is needed in which the cellular level of H1 is reduced. This has been difficult to achieve in mammals because mice contain at least eight H1 subtypes that differ in amino acid sequences and expression during development. Our previous studies showed that mice null for one or even two of the six different somatic H1 genes develop normally (Fan et al., 2001; Sirotkin et al., 1995). Apparently, the synthetic capacity of the single-copy genes encoding the different subtypes is sufficiently flexible to compensate for the lost contributions of the inactivated genes and to maintain a normal H1-to-nucleosome stoichiometry. However, we recently described a strategy for generating compound mutants in which three H1 genes have been inactivated. Embryos lacking the H1c, H1d, and H1e subtypes have about 50% the normal amount of H1, and they die by E11.5 with a very broad range of defects (Fan et al., 2003).

Therefore, in contrast to results in unicellular eukaryotes, H1 is essential for mouse development.

To begin to dissect the mechanisms by which H1 affects chromatin structure and gene transcription in vivo, we derived H1c, H1d, H1e triple null mouse embryonic stem cells (ES cells). The triple-H1 null ES cells also have a nearly 50% reduction in H1 content. We find that the marked reduction in H1 amount in these cells leads to profound changes in chromatin structure, but surprisingly, despite the global changes in chromatin structure in these cells, the expression of only a small number of genes is affected. Interestingly, a shared feature of some of these genes is that they are normally regulated by DNA methylation. The regulatory DNA regions of some of these loci are indeed hypomethylated in cells with reduced H1, even though global DNA methylation is not changed. These results indicate that, in mammals, linker histones can participate in regulating gene expression through an effect on DNA methylation.

RESULTS

Triple-H1 Null ES Cells Have Reduced Linker-Histone Content

To generate sources of chromatin that are depleted of H1 in vivo, we inactivated the linked genes for three H1 subtypes (H1c, H1d, and H1e) by three sequential gene targetings in mouse ES cells, as described previously (Fan et al., 2003). Homozygous triple-H1 null embryos die prior to E11.5, but since many embryos survive to E7.5–E9.5, we were able to derive homozygous triple null ES cells. A total of 40 blastocysts from intercrosses of heterozygotes were cultured, from which four H1c, H1d, H1e triple null ES cell lines were established. Four wild-type and three heterozygous ES cell lines were obtained and served as controls. HPLC and TOF-MS analyses of histone proteins from wild-type and triple-H1 null ES cells showed that the mutant cells have about 50% of the amount of H1 present in the wild-type ES cells (Figures 1A and 1B), similar to the reduction in H1 histone content observed in triple-H1 null embryos at later stages (Fan et al., 2003). This is equivalent to a molar ratio of only 1 H1 molecule per 4 nucleosome cores in the triple knockout ES lines (Figure 1B). Thus, these cells offer an opportunity to examine the properties of mammalian nuclei and chromatin in the presence of very low levels of linker histones.

Properties of H1-Depleted ES Cells

The four triple-H1 null ES cell lines were indistinguishable in appearance from the wild-type lines established at the same time, most of the cells appearing morphologically undifferentiated. Examination of chromosome spreads showed that most cells in these cultures have 40 chromosomes. Growth-rate measurements performed in parallel cultures indicate that, on average, the cell growth rates of triple-H1 null ES cells were similar to those of the wild-type cell lines. We also did not observe any difference in size or morphology between wild-type and triple null ES nuclei. Wild-type and mutant ES cells were reacted with an antibody that recognizes all H1 subtypes and counterstained with Hoechst dye to identify centromeric and pericentromeric heterochromatin. H1-depleted ES cells showed no changes in differential accumulation of H1 in centromeric chromatin or any other subnuclear compartment, and there was also no difference in H1 distribution along mitotic chromosomes (data not shown). Immunofluorescence examination of the intranuclear distribution of the key histone modifications H4K12Ac; H3K9Me(2); H3K27Me(3); and nonhistone proteins known to be associated with heterochromatin, such as HP1α, HP1β, and MeCP2, also revealed no significant differences in intranuclear distribution between the wild-type and H1-depleted ES cells (data not shown).

Reducing Linker-Histone Content Leads to Decreases in Nucleosome Repeat Length

Carefully controlled micrococcal nuclease digests of isolated wild-type and H1-depleted nuclei revealed that H1 depletion was accompanied by a striking ~15 bp reduction in the spacing between nucleosomes (nucleosome repeat length, NRL) from ~189 bp to ~174 bp (Figures 1C and 1D, left panels). Digestion and release conditions were selected to minimize nucleosome sliding and exchange, and the use of several time points of digestion for each batch of nuclei showed that the measured NRL changes were not an artifact due to differences in the extent of digestion. Further, the clear linear relationship between nucleosome number and DNA length permits confidence in the calculated NRL values. As discussed below, the strong correlation between NRL and total H1 per nucleosome applies both to adult mouse tissues and ES cells over a wide range of H1 content, suggesting that linker-histone availability is a primary determinant of nucleosome spacing.

Since the vast majority of the genome consists of noncoding sequences, it was possible that the observed changes in NRL were confined to this portion of the genome. We therefore examined the adenosine deaminase (*ADA*) ''housekeeping'' gene, which is transcribed at a similarly low level in both wild-type and H1-depleted cells (as determined from cDNA microarray analysis; see below). The *ADA*-specific NRL values for wild-type and H1 depleted cells (Figures 1C and 1D, middle panels) were not significantly different from the respective nucleus-wide averages. This indicates that the reduction in NRL is not confined to the noncoding portion of the genome or to heterochromatin.

As discussed below, some genes are significantly upregulated in the H1-depleted ES cells, and it was of interest to determine whether these genes exhibit similar changes in NRL. We chose to analyze the imprinting control region (ICR) of the *H19* gene because H19 RNA is significantly increased in the triple-H1 null ES cells (see below). Surprisingly, the *H19* ICR has a NRL of only 171 ± 5 bp in wild-type ES cells, significantly lower than the bulk and *ADA*-specific NRL values in these cells (Figures 1C and 1D, right panels). Furthermore, in triple-H1 null cells, in which *H19* gene expression is upregulated 7-fold, the NRL was 165 ± 5 bp, a value comparable to the NRL of yeast that lacks a canonical H1. We also noted that the *H19* ICR signal on the blots showed fewer clearly

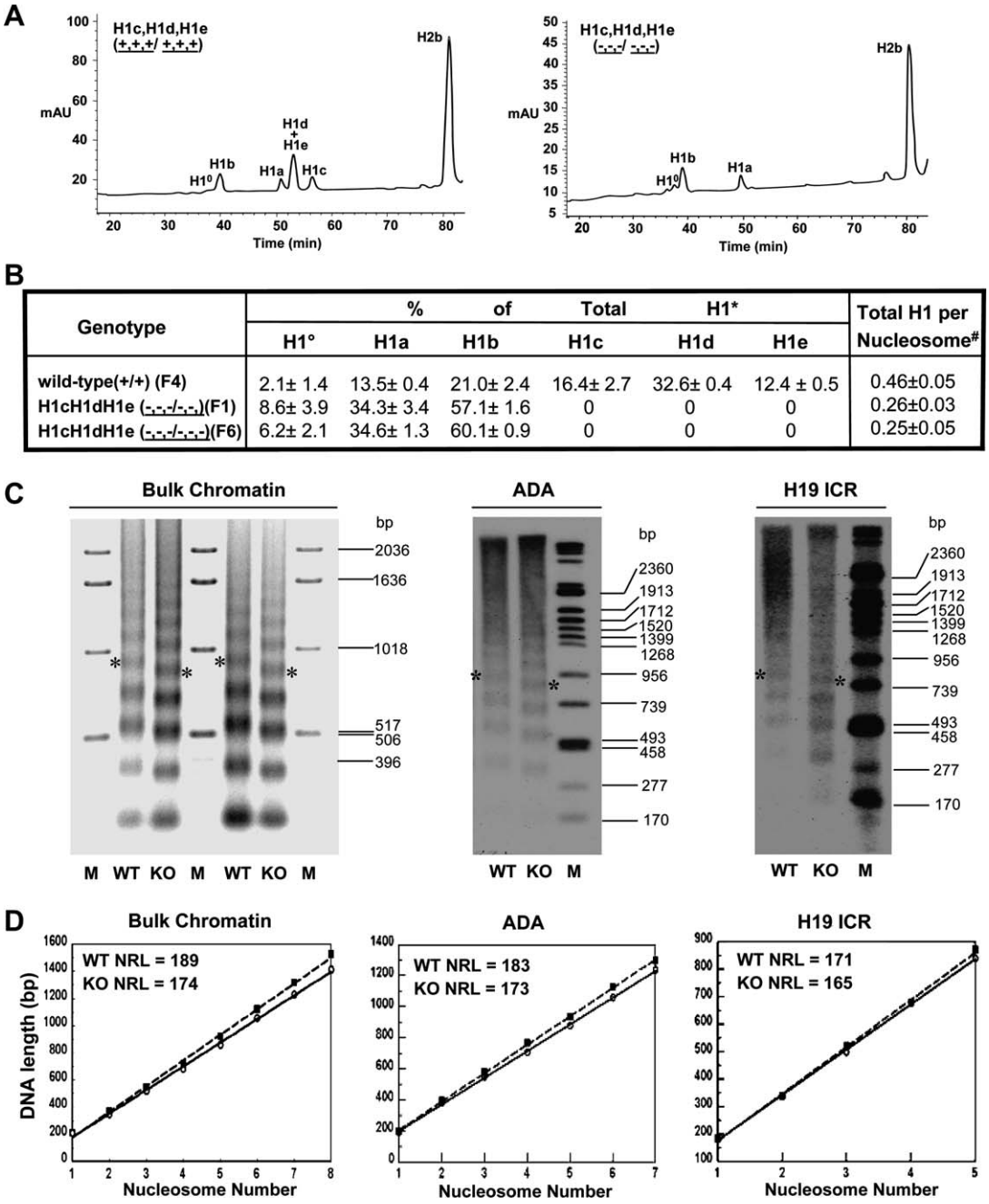

Genotype	% of Total H1*						Total H1 per Nucleosome#
	H1°	H1a	H1b	H1c	H1d	H1e	
wild-type(+/+) (F4)	2.1± 1.4	13.5± 0.4	21.0± 2.4	16.4± 2.7	32.6± 0.4	12.4 ± 0.5	0.46±0.05
H1cH1dH1e (-,-,-/-,-,-)(F1)	8.6± 3.9	34.3± 3.4	57.1± 1.6	0	0	0	0.26±0.03
H1cH1dH1e (-,-,-/-,-,-)(F6)	6.2± 2.1	34.6± 1.3	60.1± 0.9	0	0	0	0.25±0.05

Figure 1. Reduced H1 Content in Triple-H1 Null ES Cells Leads to Reduced Nucleosome Spacing

(A) Reverse-phase HPLC analysis of approximately 20 μg of total histone extract of chromatin from wild-type (left) and homozygous H1c, H1d, H1e mutant ES cells (right) performed as described previously (Fan et al., 2001). mAU, milliabsorbency units at 214 Å.

(B) H1 subtype composition of chromatin from wild-type and *H1c*$^{-/-}$*H1d*$^{-/-}$*H1e*$^{-/-}$ ES cells. Data were calculated from HPLC analyses like that shown in (A). Values are means ± standard deviations of individual determinations of three histone preparations from each cell line. The percentage of total H1 and total H1 per nucleosome were determined as described previously (Fan et al., 2003).

(C) Nucleosome repeat length (NRL) from bulk chromatin (left panel), *ADA* locus (middle panel), and *H19* ICR region (right panel). Paired lanes of MNase digests of nuclei from wild-type (WT) and triple-H1 null (KO) ES cells. M, DNA markers with sizes of prominent bands labeled (bp, base pairs). The penta-nucleosome bands are identified by asterisks. For bulk chromatin (left panel), in the first pair of lanes, the digestion of wt nuclei is more extensive than that of the KO nuclei, while in the second pair, the digestion of KO nuclei is more extensive. The KO oligonucleosome bands migrate faster under both conditions.

(D) Plot of nucleosome number versus DNA length for ES cell bulk chromatin (left panel), *ADA* locus (middle panel), and *H19* ICR region (right panel) shown in (C). Symbols show the data points, and lines are the linear regressions of the data points. Solid square symbols and dashed lines are for wt ES cells; open circles and solid lines are for H1 triple null ES cells. (see Experimental Procedures for details). The NRL values are indicated.

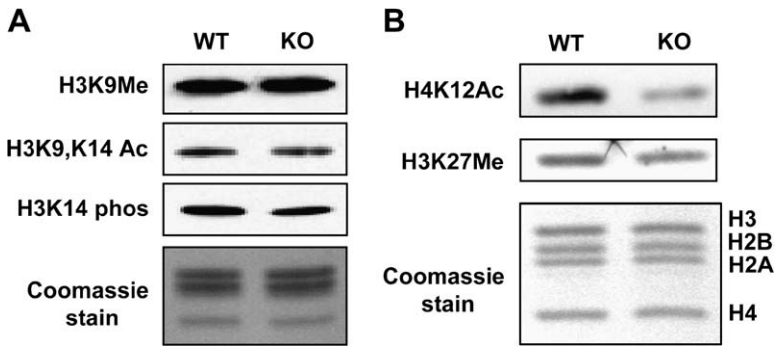

Figure 2. Reduced H1 Content Leads to Reduced Levels of Certain Histone Modifications

Ten micrograms of nuclear histone extracts were analyzed by immunoblotting with antibodies specific for the indicated histone modifications. Representative immunoblots are shown. Experiments were repeated twice with multiple cell lines. The average reduction in H4K12Ac was 4-fold, and the average reduction in H3K9 dimethylation was 2-fold. The bottom panels in (A) and (B) show gels stained with Coomassie blue, indicating equal loading of proteins from wild-type (WT) and triple-H1 null (KO) ES cells.

defined bands than the signal from either the bulk DNA or the *ADA* gene. A difference in nucleosome ladder definition between euchromatin and heterochromatin has been observed before (Berkowitz and Riggs, 1981; Sun et al., 2001), suggesting a more irregular nucleosome distribution in the former. To assess the H1 content of chromatin in the vicinity of the *H19* ICR and the *ADA* gene, we carried out quantitative chromatin immunoprecipitation (qChIP) experiments in wild-type and triple-H1 null ES cells. The results show that these two regions contain about one-half as much H1 in the mutant cells as compared to the wild-type cells (see Figure S1 in the Supplemental Data available with this article online), consistent with the extent of bulk H1 depletion measured by HPLC. Interestingly, the H1 content in the region around the *H19* ICR appears to be significantly less than that at the *ADA* gene in both wild-type and mutant ES cells, consistent with the comparative NRL measurements in these two regions (Figure 1). The foregoing NRL measurements of bulk and specific single-copy gene chromatin provide in vivo evidence that H1 influences nucleosome spacing in both the heterochromatic and euchromatic compartments of the nucleus.

The Levels of Two Key Histone Modifications Are Altered in Linker-Histone-Depleted Nuclei

As noted above, H1-depleted cells show no qualitative differences in the intranuclear distribution of H1 or several key core histone modifications. However, it was possible that the relative quantities of core histone modifications were altered in the compound H1 null nuclei. To address this issue, semiquantitative Western blotting with modification-specific antibodies was used to determine the relative levels of several histone modifications in the triple-H1 null ES cells and wild-type littermate ES cells. While the levels of most modifications remain unchanged in triple KO ES cells compared to wild-type controls (Figure 2A), the depletion in total H1 did result in a reproducible ~4-fold reduction in H4 K12 acetylation and a moderate ~2-fold reduction in H3 K27 trimethylation (Figure 2B). The dramatic decrease of H4K12Ac in H1-depleted nuclei effectively increases the neutralization of DNA negative charges in the nucleus and thus tends to create a more compact chromatin. Reduction in both H4K12Ac levels and NRL will therefore have an additive effect in compensating for H1 loss.

H1 Depletion Results in Local Reductions in Chromatin Compaction

The above results all point to the effects of H1 depletion on chromatin structure being nucleus-wide rather than confined to any specific nuclear compartments or genes. However, these approaches do not address the question of the distribution of H1 at the local chromatin-fiber level, where its influence on chromatin architecture and conformation in vitro has been studied extensively (van Holde, 1989; Wolffe, 1998). In vitro, H1-depleted oligonucleosomes sediment more slowly and fail to adopt the zigzag conformation or fold into the 30 nm fibers characteristic of native chromatin (Bednar et al., 1998; Thoma et al., 1979). However, it has not previously been possible to determine the structural impact of partial H1 loss on chromatin assembled in vivo. Polynucleosomes (n = 20–40) from wild-type and triple-H1 knockout ES cells were analyzed by electron microscopy. A clear difference in polynucleosome conformation between wild-type and triple-H1 knockout chromatin was seen when the chromatin was equilibrated in 25 mM NaCl (Figure 3A). The H1-depleted chromatin appeared less compact and more variable in conformation. When the differences were quantitated by scoring the frequency of four arbitrary levels of compaction, a striking conformational difference was revealed (Figure 3B). Oligonucleosomes from H1-deficient ES cells were much less compact than those from wild-type ES cells, as judged by the proportion containing either an open, ''beads-on-a-string'' conformation (increased in mutant) or a more compact chromatin-fiber-like conformation (decreased in mutant). Some polynucleosomes exhibited more than one level of compaction, with, e.g., visible linker in one region and a chromatin-fiber conformation in another (Figure 3A, arrows). This level of irregularity is rarely seen in chromatin with H1 levels close to 1 molecule per nucleosome (Bednar et al., 1998; Thoma et al., 1979; Zlatanova and Doenecke, 1994). Importantly, these observations indicate that conditions of reduced H1 availability in vivo result in short-range heterogeneity in linker-histone distribution rather than extended regions of H1-free chromatin interspersed with H1-containing nucleosomes.

Reduced H1 Content in ES Cells Leads to Highly Specific Changes in Gene Expression

As described above, the 50% reduction in H1 content produced by inactivating three H1 genes caused very marked

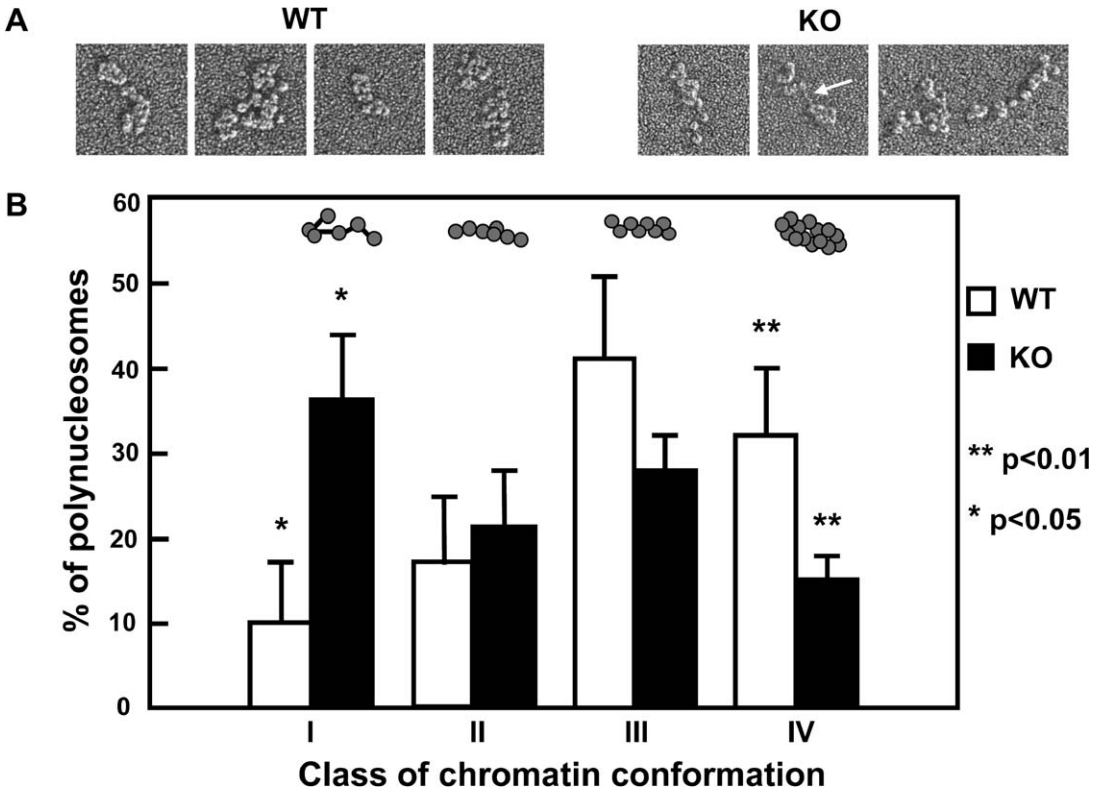

Figure 3. Reduced H1 Content Causes Chromatin-Fiber Decondensation

(A) Images of polynucleosomes (n = 20–40) isolated from wild-type (WT, left) and H1c, H1d, H1e triple homozygous null (KO, right) ES cells by micrococcal nuclease digestion and shadowed with platinum as described previously (Georgel et al., 2003). Images are shown in reverse contrast. Many of the polynucleosomes have conformations that change along their length (arrow). This heterogeneity is especially striking in polynucleosomes from mutant cells.

(B) Classification of polynucleosomes in the micrographs according to the conformation types depicted above the bar graphs. H1-deficient chromatin has a much larger proportion of open chromatin with linker DNA visible, while the "30 nm fiber" conformation is more common in the wild-type (see text). In cases in which more than one conformation type was present in a polynucleosome, each type was included in the bar chart. Error bars represent one standard error of the mean.

changes in the properties of bulk chromatin. Therefore, it was of great interest to determine how the changes in chromatin structure affected gene expression throughout the genome. We compared the gene-expression profile of 12,489 different sequences representing approximately 6,000 genes and 6,000 ESTs by hybridization of biotin-labeled antisense RNA (cRNA) from triple-H1 null and wild-type littermate ES cells to Affymetrix U74Av2 microarrays. We chose to compare ES cells rather than embryos in these experiments because in the undifferentiated state, ES cells represent a homogenous cell type and because the triple-H1 null embryos exhibited a wide range of phenotypic defects (Fan et al., 2003). To avoid potential variations among ES cell lines, we analyzed gene-expression patterns in several ES cell lines derived from littermate male embryos produced from matings of N7 backcrossed C57Bl6 triple heterozygous H1 mutant parents.

Despite the global changes in chromatin structure present in the triple-H1 null ES cells, they exhibited very few gene-expression changes when compared with wild-type ES cells (Figure S2 and Table 1). Among the 12,489 target probe sets assayed, 6,842 targets showed significant expression in at least one of the ES cell lines. These 6,842 expressed sequences represent 4,450 distinct known genes (Table 2). The results showed that only 38 targets (0.56%) have expression differences ($p \leq 0.05$) of 2-fold or more in the triple-H1 null ES cells compared with wild-type littermate ES cell controls (Table 2). Table 1 presents a list of the 29 known genes in this group. Among these 29 genes, there were 19 with increased expression and 10 with decreased expression, indicating that reduction of H1 content has both positive and negative effects on gene expression. Nevertheless, there are more upregulated genes than downregulated genes in the triple KO ES cells, and the largest changes are among the upregulated gene group. We performed Northern blot hybridization and/or RT-PCR analysis to confirm several of the gene-expression changes, including those for H19 and Igf2 (Figure 4A); $H1^0$ and Pem (Figure 4B); and H1Fx, Gtl2, and Xlr3 (data not shown). Quantitation of changes in mRNA levels observed on Northern blots using phosphorimaging and ImageQuant software was, in all cases, in excellent agreement with

Table 1. Genes with Altered Expression in Triple-H1 Null ES Cells

Accession Number	Entrez Definition	Average Fold Change[a]	Chromosomal Location
Genes with Increased Expression in Triple-H1 Null ES Cells[a]			
L22977	*Mus musculus* A12 gene, two nearly identical genes, XLR3a and Xlr3b (X-linked lymphocyte regulated)	10.3	X
Y13832	*Mus musculus* mRNA for GT12 protein	9.1	12
X58196	*Mus musculus* H19 mRNA	7.1	7
AJ006584	*Mus musculus* mRNA for translation initiation factor eIF2 gamma Y-linked	6.4	Y
M32484	*Mus musculus* placenta and embryonic expression early gene (pem) mRNA, complete cds	4.6	X
M80631	Mouse G protein alpha subunit (GNA-14) mRNA, complete cds	4.4	19
M29260	Mouse histone 1-0 gene, 5′ end, and promoter region	4.0	15
M55413	*Mus musculus* vitamin D-binding protein (GC) mRNA, partial cds	3.2	5
M20625	Mouse testis-specific cytochrome c mRNA	2.9	2
AJ007376	*Mus musculus* mRNA for DBY RNA helicase	2.8	Y
X05546	Murine (DBA/2) mRNA fragment for gag related peptide	2.8	[b]
X03505	Mouse gene exon 2 for serum amyloid A (SAA) 3 protein	2.7	7
AF017453	*Mus musculus* homeobox protein PSX mRNA, complete cds	2.6	X
NM019703	*Mus musculus* phosphofructokinase, platelet (Pfkp), mRNA	2.6	13
AI851599	ESTs, weakly similar to H1.4_MOUSE histone H1.4 (H1 VAR.2) (H1E) [*Mus musculus*] (putative ortholog H1x)	2.5	6
D88539	*Mus musculus* mRNA for synaptonemal complex protein 1, partial cds	2.4	3
AF068182	*Mus musculus* B cell linker protein BLNK mRNA, complete cds	2.1	19
X69832	*Mus musculus* mRNA for serine protease inhibitor 2.4	2.1	12
X04120	*Mus musculus* intracisternal A-particle IAP-IL3 genome deleted type I element inserted 5′ to the interleukin-3 gene	2.0	[b]
Genes with Decreased Expression in Triple-H1 Null ES Cells[a]			
X71922	*Mus musculus* gene for IGF-II, exon 6	3.1	7
AF090738	*Mus musculus* insulin receptor substrate-2 (Irs2) gene, partial cds	2.5	8
NM 023422	*Mus musculus* H2B histone family, member S (H2bfs), mRNA	2.4	13
M12481	Mouse cytoplasmic beta-actin mRNA	2.2	5
X95504	*Mus musculus* zinc finger protein regulator of apoptosis and cell cycle arrest (Zac1), mRNA	2.2	10
K02245	Mouse proliferin mRNA, complete cds	2.2	13
AF009366	*Mus musculus* neural precursor cell expressed developmentally downregulated Nedd9 (Nedd9) mRNA, complete cds	2.1	13
AJ132098	*Mus musculus* mRNA for Vanin-1	2.1	10
U41465	*Mus musculus* BCL-6 mRNA, complete cds	2.0	16
L33779	*Mus musculus* desmocollin type 2 (DSC2) mRNA, complete cds, alternatively spliced	2.0	18

[a] Genes listed have increased or decreased expression $\geq$2-fold in triple-H1 null ES cells versus wild-type ES cells ($p \leq 0.05$).
[b] Target sequences are present at multiple chromosomal locations.

Table 2. Summary of Affymetrix Microarray Analysis of Gene Expression in ES Cells

MG_U74Av2	Total	Number of Imprinted Genes (% Total)	Number of X-Linked Genes (% Total)	Number of Y-Linked Genes (% Total)	Number of Genes up ≥2-fold (% Total)	Number of Genes down ≥2-fold (% Total)
Total probe sets	12,489	33 (0.26%)	214 (1.71%)	13 (0.10%)	25 (0.20%)	13 (0.10%)
Number of expressed probe sets	6,842	23 (0.34%)	115 (1.68%)	4 (0.06%)	25 (0.37%)	13 (0.19%)
Number of expressed probe sets from known genes[a]	5,259	23 (0.44%)	112 (2.13%)	4 (0.08%)	21 (0.40%)	11 (0.21%)
Number of distinct expressed known genes[a]	4,450	*22 (0.49%)*	*92 (2.07%)*	*4 (0.09%)*	19 (0.43%)	10 (0.22%)
Number of known genes with altered expression ≥2-fold[b]	29	*4 (13.8%)*	*3 (10.3%)*	*2 (6.90%)*	19 (65.5%)	10 (34.5%)

[a] The number of expressed sequences was determined by counting probe sets that have present (P) calls from at least one cell line.
[b] The number of distinct known genes with decreased or increased expression in triple-H1 null ES versus wild-type ES cells ($p \leq 0.05$).

the fold changes in expression measured by microarray analysis.

Examination of the 29 genes listed in Table 1 leads to both expected and unexpected findings. Based upon the results shown in Figures 1A and 1B, it might be expected that the mRNA for H1°, the replacement linker histone, would be increased in the triple-H1 null ES cells since HPLC analysis showed that the protein was increased near 3-fold in these cells. Indeed, H1° mRNA is increased 4-fold in the triple null cells (Table 1 and Figure 4B).

Strikingly, among the 29 known genes with altered expression in the triple null ES cells, four are imprinted genes (*H19*, *Igf2*, *Gt12*, and *Zac1*). There are about 70 imprinted genes described to date (http://www.mgu.har.mrc.ac.uk), 33 of which were present on the array and 22 of which were expressed in the ES cells (Table 2). These imprinted genes represent only 0.49% of the known expressed genes on the array, and yet they represent 13.8% (4 of 29) of the genes exhibiting expression changes in the triple-H1 null ES cells. Clearly, imprinted genes are overrepresented among the genes that are sensitive to reduced H1 levels. Furthermore, they are among the most dramatically affected (Table 1).

Many imprinted genes occur in clusters, and sometimes genes within such clusters are reciprocally expressed from the two parent-derived chromosomes. The *H19* and *Igf2* genes are the best studied examples of reciprocal imprinted expression. *H19* is generally not expressed in undifferentiated ES cell lines (Tucker et al., 1996). We examined two wild-type ES cell lines and found that neither had significant levels of H19 RNA but that both expressed Igf2 mRNA. In contrast, all four triple-H1 null ES lines studied expressed substantial levels of H19 RNA, and all of these lines exhibited reduced Igf2 mRNA levels (Figure 4C and data not shown). Interestingly, two ES cell lines heterozygous for the three null H1 alleles also had elevated levels of H19 RNA compared with wild-type ES cells; these levels appeared to be somewhat lower than those in triple null ES cells.

Another group of related genes, the sex-chromosome genes, is also overrepresented among the genes with altered expression in the triple null ES cells. Five (17%) of the twenty-nine genes with altered expression are located on the X and Y chromosomes, even though only 2.07% and 0.09%, respectively, of the known genes on the array are on these two chromosomes (Table 2). These differences in expression are not attributable to differences in sex-chromosome content of the ES cell lines since only ES cell lines derived from male embryos were used, as determined by genotyping for the *Sry* gene on the Y chromosome of ES cells (data not shown). Interestingly, all of these genes are upregulated in the triple-H1 null ES cells, and several of them are among the genes with the highest degree of change.

Reduced H1 Content in Embryonic Cells Leads to Reduced DNA Methylation Specifically within the Imprinting Control Regions of the *H19-Igf2* and *Gtl2-Dlk1* Loci

The results presented in the preceding section show that nearly one-third of the genes with altered expression in the triple-H1 null ES cells are imprinted genes or genes located on the X and Y chromosomes. DNA methylation plays an important role in regulating expression of both categories of genes. Four of the genes in Table 1 (*H19*, *Igf2*, *X1r3*, and *Pem*) were also reported to exhibit altered expression in fibroblasts deficient for Dnmt1, a major maintenance DNA methyltransferase (Jackson-Grusby et al., 2001). Furthermore, another transcript shown in Table 1 is derived from a gene inserted with an IAP provirus (X04120) that occurs many times in the mouse genome. These types of sequences are often silenced by DNA methylation. Upregulation of IAP transcripts in the triple null ES cells was confirmed by Northern blot hybridization (data not shown). Taken together, all of these results suggested that the reduced H1 content in the triple null ES cells may have led to changes in DNA methylation. To investigate this possibility, we compared wild-type and triple-H1 null ES cells for the overall level

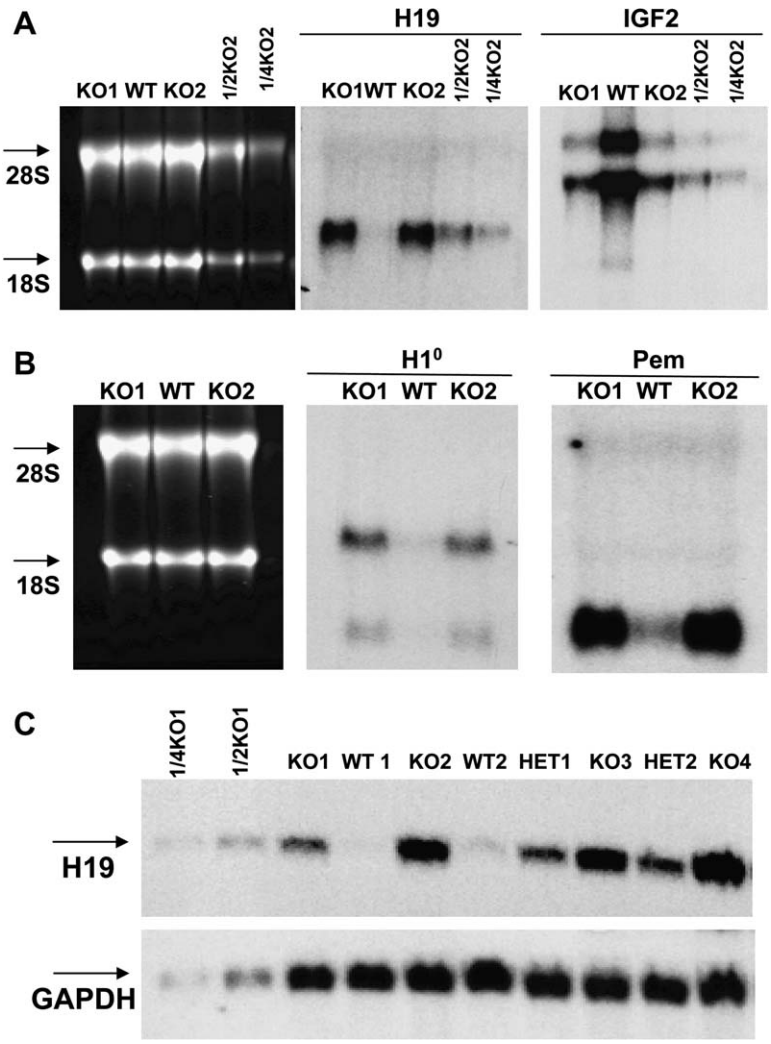

Figure 4. Northern Blot Analysis of Selected Genes

(A and B) Twenty micrograms of RNA from wild-type (WT) or two H1c, H1d, H1e triple null ES cell lines (KO1 and 2) were analyzed by Northern blot hybridization with probes specific for H19 ([A], middle panel), IGF2 ([A], right panel), H1° ([B], middle panel), or Pem ([B], right panel). The left panels in (A) and (B) show the ethidium-bromide-stained gels.

(C) H19 RNA levels in multiple ES cell lines were determined by Northern blot hybridization. The level of GAPDH RNA served as a loading and transfer control. The two right lanes in (A) and two left lanes in (C) were loaded with the indicated dilutions of RNA to demonstrate that hybridization intensities were in the linear range.

of genomic DNA methylation, as well as the extent of DNA methylation at specific repetitive sequences and at two loci (*H19-Igf2* and *Gtl2-Dlk1*) where the genes exhibited an altered expression pattern in the triple null ES cells.

Digestion of total genomic DNA with MspI and the methylation-sensitive isoschizomer HpaII, which recognize CCGG sequences, did not reveal a difference in genomic DNA methylation between the two types of ES cells (Figure 5A). Digestion with another methylation-sensitive enzyme, MaeII, which recognizes ACGT sequences, also did not show a difference (Figure 5A). Digestion with MspI or HpaII, followed by Southern blot hybridization with a probe specific for the mouse minor satellite repeat (Lehnertz et al., 2003), did not show a difference in these sequences that are present as 50,000–100,000 copies localized in centromeric regions (Kalitis and Choo, 1989) (Figure 5B). Likewise, using MaeII digestion and a probe specific for the mouse major satellite repeat, we did not see a substantial difference in the degree of methylation of the major satellite repeat of about 700,000 copies in pericentric regions (Hastie, 1989), although there appears to be a slight decrease in sensitivity to MaeII digestion in the two triple-H1 null lines, possibly reflecting a slight increase in methylation of these sequences with reduced H1 content (Figure 5C). We also did not detect a difference in DNA methylation of endogenous C type retrovirus repeats (Li et al., 1992) (Figure 5D). Thus, reduction of H1 content in ES cells does not appear to affect overall genomic DNA methylation or that of several types of highly methylated, repetitive sequences.

We next studied the *H19-Igf2* and *Gtl2-Dlk1* loci, where parent-of-origin-specific DNA methylation patterns have been shown to regulate expression of the genes (Reik and Walter, 2001; Schmidt et al., 2000; Verona et al., 2003). A key regulatory element controlling the reciprocal expression of the *H19* and *Igf2* genes is the ICR located between *Igf2* and *H19*, 2–4 kb upstream of *H19* (Reik and Murrell, 2000). The mouse *H19-Igf2* ICR contains four binding sites for a protein factor called CTCF that, when bound there, is thought to insulate the *Igf2* promoter from the transcriptional enhancing activity of sequences downstream of *H19* (Bell and Felsenfeld, 2000; Hark et al., 2000). DNA binding by CTCF is inhibited by DNA methylation. In undifferentiated

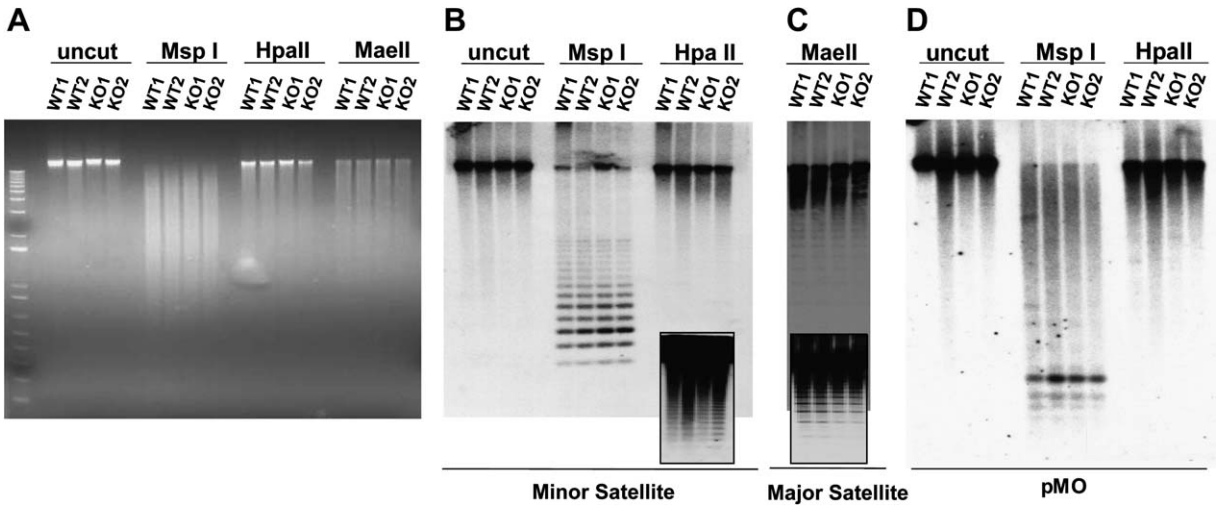

Figure 5. Global DNA Methylation Is Not Altered in Triple-H1 Null ES Cells

(A) Genomic DNA from two H1c, H1d, H1e null ES cells (KO1 and KO2) and two wild-type ES cell lines (WT1 and WT2) was digested with either MspI, HpaII, or MaeII and then separated by agarose-gel electrophoresis. DNA was visualized by ethidium-bromide staining.

(B–D) DNA blots from (A) were hybridized with probes specific for minor satellite repeats (B), major satellite repeats (C), or endogenous C type retroviruses (pMO) (D). The inserts in the lower part of (B) and (C) are longer exposures that show the digested (unmethylated) DNA fragments.

ES cells, however, *H19* is not expressed from either chromosome (Poirier et al., 1991; Tucker et al., 1996). Since we observed a reciprocal change in expression of *Igf2* and *H19* transcripts in triple-H1 null ES cells compared to wild-type ES cells, we analyzed DNA methylation of the ICR by bisulfite sequencing, which allows quantitative determination of the methylation status of each cytosine in a given DNA sequence (Clark et al., 1994). We performed bisulfite pyrosequencing on a region of the ICR from nt 1447 to 2124 (GenBank accession number AP003183) that includes two CTCF binding sites (Bell and Felsenfeld, 2000; Hark et al., 2000). In agreement with previously published results (Dean et al., 1998; Li et al., 1993; Tucker et al., 1996; Warnecke et al., 1998), we found that most CpG dinucleotide sequences in this region are predominantly methylated in wild-type ES cells. In contrast, the extent of methylation of the CpGs in CTCF binding site 1 is significantly lower in the triple-H1 null ES cells (Figure 6A and Figure S3). Similar results were obtained at CTCF binding site 2 (data not shown). The results for CTCF binding site 1 were confirmed by ClaI digestion of bisulfite-treated and amplified DNA (data not shown).

Like *H19*, expression of the *Gtl2* gene is significantly upregulated in H1 triple KO ES cells compared to wild-type cells (Table 1). The *Gtl2-Dlk1* region is a recently characterized imprinted domain that shares several common characteristics with the *H19-Igf2* locus, including parent-of-origin differentially methylated regions (DMRs) (Lin et al., 2003; Takada et al., 2002). Bisulfite sequencing showed that the extent of CpG methylation is reduced at the *Gtl2* DMR region (Figure 6B) and the intergenic germline-derived DMR (IG-DMR) region in triple-H1 null ES cells (Figures 6C and 6D). In contrast, the extent of CpG methylation is unchanged at two loci, the promoter regions of the α-*actin* gene and the alkaline myosin light chain (*Myl-c*) gene (Oswald et al., 2000), where transcription is not altered in the mutant ES cells (Figures 6E and 6F). Control experiments were performed with E9.5 DNA and DNA from Dnmt1 null ES cells to demonstrate the accuracy of the bisulfite DNA pyrosequencing procedures (Figure S4). Methylation at cytosine dinucleotides other than CpG was relatively rare, and the frequency of methylation at these sites was not changed in the mutant cells (data not shown). Thus, reducing the H1 amount in ES cells leads to quantitative reductions in the extent of DNA methylation at specific CpG dinucleotides.

DISCUSSION

Previous work on the linker histones has suggested that they have two interrelated functions, as chromatin architectural proteins and as transcriptional repressors. However, much of the data used to infer these functions has been derived from in vitro studies. These concepts also need to be reevaluated in the light of the minimal effects of H1 deletion in unicellular eukaryotes and depletion in a few selected systems from higher organisms (reviewed in Harvey and Downs, 2004; Thomas, 1999). The triple-H1 null mouse embryonic stem cells established in the present study provide an opportunity to examine the in vivo influence of H1 on both chromatin architecture and the transcriptional repertoire in a vertebrate system.

Effects of H1 on Nuclear Structure and Chromatin Architecture

The most striking effect of H1 depletion on chromatin structure was a consistent reduction in nucleosome repeat length, which was observed both globally and locally in the *ADA* "housekeeping" gene and in the *H19* ICR (Figure 1). One consequence of a change in NRL is a change in the

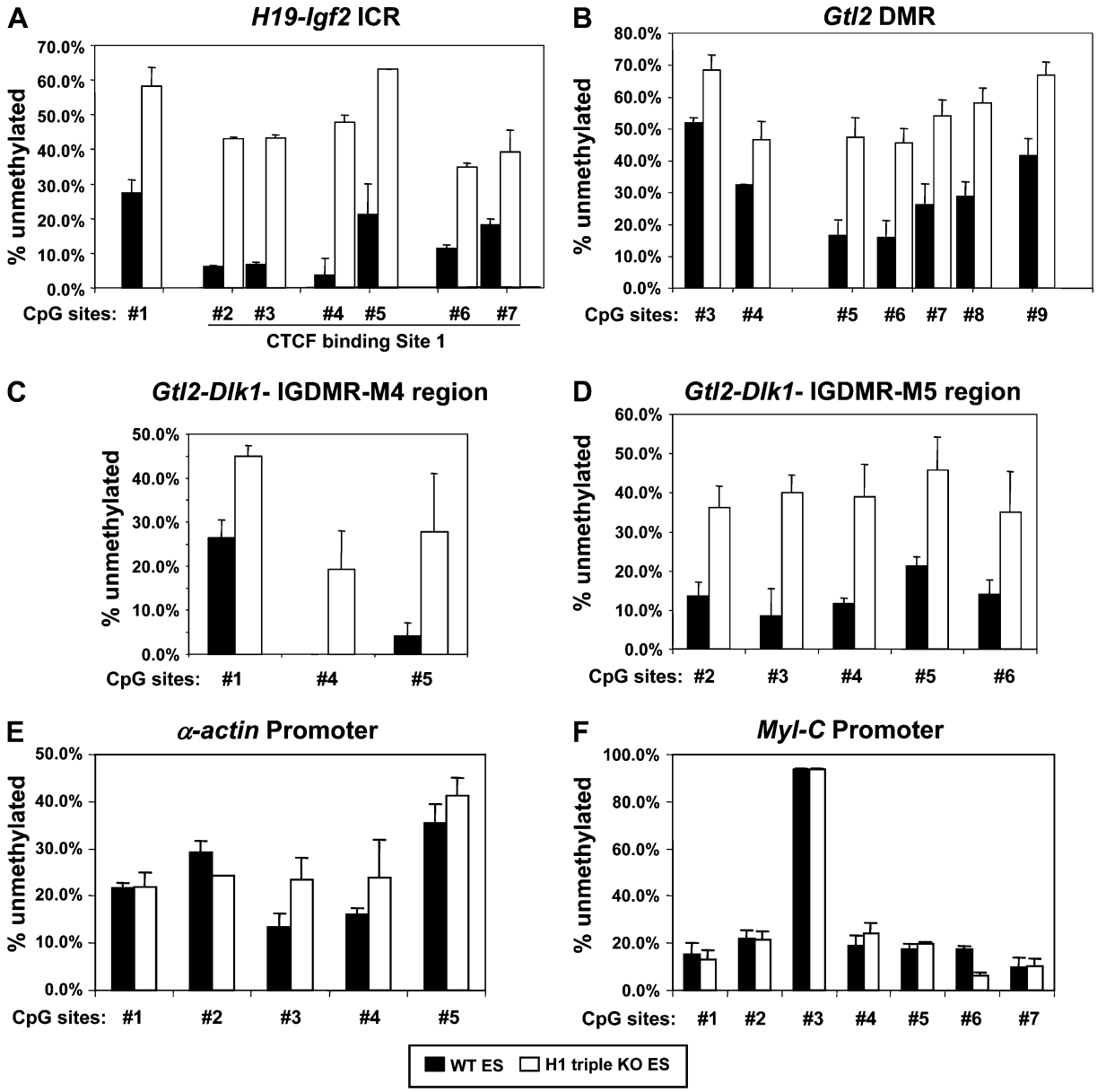

Figure 6. Reduction of H1 Content Leads to Reduced Methylation of CpGs in the Imprinting Control Regions of *H19-Igf2* and *Gtl2-Dlk1* Loci

Pyrosequencing of bisulfite-treated DNA isolated from wild-type (WT) ES cells and triple-H1 null ES cells was performed over the indicated regions as described in Experimental Procedures. The primer sequences and chromosomal regions analyzed are shown in Table S1. The percentage of DNA strands that are unmethylated was determined from pyrosequencing analyses like those shown in Figure S3. The results show representative analyses performed on two independently isolated wild-type ES lines and two independently isolated triple-H1 null ES lines. Error bars indicate the standard deviations for two ES cell lines. The percent of CpG methylation did not change appreciably with cell-line passage number. Control experiments were performed on the same regions with bisulfite-treated DNA from E9.5 wild-type embryos and Dnmt1 null ES cells (Figure S4).

charge balance within the nucleus as it effectively removes free (linker) DNA from the system. Based on the dominant effect of electrostatic-charge interactions on chromatin conformation (Clark and Kimura, 1990), it seems possible that the change in charge balance caused by reduction in total H1 content is balanced by a concomitant reduction in NRL. We examined the relationship between H1 content and NRL using the ES cell data presented here (Figure 1) together with results on H1-depleted differentiated cells from mature mouse tissues reported earlier (Fan et al., 2003). We find a robust linear relationship between NRL and H1/nucleosome (linear regression $r^2 = 0.95$) over the range

from 0.25 to 0.80 H1 per nucleosome (Woodcock et al., 2006). The slope of the line indicates that, for example, the nucleus-wide addition of 1 H1 molecule/nucleosome would, on average, result in an increase of ~37 bp in NRL. Viewed in terms of charge balance, 37 bp of double-stranded DNA represents 74 negative charges, while vertebrate H1s typically have ~60 K+R positively charged residues, indicating a fairly close correspondence between these two parameters. The 4-fold reduction of acetylated lysine 12 on H4 that we observed in the H1-depleted nuclei will also effectively contribute to the restoration of charge balance.

Our detailed measurements of H1 stoichiometry in both ES cells and mature differentiated cells also prompt a reconsideration of the generalization that there is ''about'' 1 H1 per nucleosome in most eukaryotic nuclei. In fact, in the wild-type mouse cells where this has been examined, the stoichiometry varies from tissue to tissue but is consistently less than 1 per nucleosome (Fan et al., 2003). This has important implications since, at any given moment, a significant proportion of nucleosomes will lack H1, exposing sites for the binding of other proteins to the linker DNA and the linker entry/exit region of the nucleosome. Even in the case of quiescent mouse splenocytes, with ~0.8 H1 molecules per nucleosome (Fan et al., 2003), individual nucleosomes will be H1-free 20% of the time, the only exceptions being in the small portion of the genome that may have firmly bound H1 (Misteli et al., 2000). It is also apparent that linker-histone stoichiometry is generally correlated with the extent of cell differentiation, with quiescent splenocytes having the highest H1 stoichiometry and pluripotent ES cells the lowest among the wild-type mouse cells we examined.

In light of the viability of cells with low H1-per-nucleosome ratios, how should the extensive body of data on H1 as a chromatin architectural protein be viewed? Clearly, in nuclei with 1 H1 per 4 nucleosomes, H1-directed zigzag structures (Thoma et al., 1979) must play a more minor role in the overall conformation of chromatin than in systems with close to 1 H1 per nucleosome, and this would be predicted to result in less regular chromatin fibers (Bednar et al., 1998; Carruthers et al., 1998). In fact, isolated oligonucleosomes from ES cells (Figure 3) are more irregular in diameter and overall conformation than those observed in chicken erythrocytes and other chromatins with higher H1 content (e.g., Williams et al., 1986; Woodcock et al., 1991). Moreover, the degree of compaction in ES oligonucleosomes, while locally highly variable, on average shows a decrease at lower H1 levels (Figure 3B). It is well established in vitro that, in the absence of H1, chromatin compacts in response to the electrostatic interactions induced by mono- and divalent cations (Schwarz and Hansen, 1994). Compaction in the absence of H1 is dependent on the N termini of the core histones (Allan et al., 1982; Dorigo et al., 2003; Fletcher and Hansen, 1996). In this respect, the decreased acetylation of H4 at lysine 12 that we observe in H1-depleted ES cells would tend to further counteract the loss of H1 and restore charge homeostasis, a conclusion supported by the finding that core histone acetylation inhibits H1-mediated chromatin compaction in vitro (Ridsdale et al., 1990).

Effects of H1 on Gene Expression

Linker histone H1 has long been regarded as a general repressor of transcription. This view is consistent with the properties of H1, especially its ability to stabilize higher-order chromatin structure (Thomas, 1999; Wolffe, 1998), which is expected to limit access of transcriptional activators to DNA. Various types of studies have shown that transcriptionally active chromatin contains less H1 than transcriptionally inactive regions (reviewed in Zlatanova and Van Holde, 1992). However, these correlative observations do not establish whether removal of H1 is a prerequisite for gene activation.

To begin to investigate the role of H1 in regulating gene transcription in vivo, we and others have developed methods for manipulating the level of H1 in cells. Elimination of H1 in *Tetrahymena* did not cause changes in the total amounts of the several categories of cellular RNAs, suggesting that loss of H1 does not cause increases in transcription by the three types of RNA polymerases (Shen and Gorovsky, 1996). Deletion of the yeast *HHO1* gene encoding the putative linker histone also did not lead to significant (>50%) increases in gene expression (Hellauer et al., 2001). Instead, a modest decrease in expression of a very small number of genes was seen. Thus, studies in these unicellular eukaryotes do not support the view that H1 is a repressor of global transcriptional activity. However, H1 is not essential for viability in either of these organisms, and both H1 proteins have a structural organization rather different from those of metazoan linker histones. Therefore, it was of great interest to determine how a reduction in linker histone H1 affects the gene-expression pattern in mammalian cells.

Despite the striking changes in chromatin structure in the triple KO ES cells, we found very few genes that differed in expression level by 2-fold or more. Unlike the results obtained in yeast, examples of both increased and decreased expression were seen in the H1-depleted ES cells. However, as in yeast, the magnitude of decreased expression changes was rather modest, whereas in the triple-H1 null cells, several genes were strongly upregulated. Thus, H1 is clearly not a repressor of global transcriptional activity in mammalian cells, and, in general, our results agree with the analyses in *Tetrahymena* and yeast. Instead, H1 appears to be involved in regulating the expression of specific genes, even though our other results clearly show that its depletion affects fundamental aspects of chromatin structure throughout the genome.

In contrast to the studies in yeast, in which no common features of the H1-sensitive genes were found, our results identify a category of genes whose expression is especially sensitive to H1 content. Nearly one-third of the genes with altered expression in the H1-depleted cells are thought to be normally regulated by DNA methylation. Importantly, 4 of the 29 known genes (*Xlr3*, *Pem*, *H19*, and *Igf2*) identified in our study have an altered expression in mouse embryonic fibroblasts deficient for Dnmt1, the major maintenance DNA methyltransferase in mammalian cells (Jackson-Grusby et al., 2001). We measured the level of DNA methylation within the *H19-Igf2* imprinting control region (ICR) that

regulates the reciprocal expression of the two genes at this locus. The analysis showed that many of the CpG dinucleotides in this region were undermethylated in H1-depleted ES cells compared with control ES cells. This observation, along with our finding that expression of *H19* is upregulated and that of *Igf2* is downregulated in the H1-depleted cells, is entirely consistent with the current model for control of the two genes by the ICR (Reik and Murrell, 2000). We also found reduced CpG methylation within several DMRs at the *Gtl2-Dlk1* imprinted locus, and the expression of *Gtl2*, like *H19*, is significantly upregulated in H1-depleted cells. The effect of H1 depletion on DNA methylation within the imprinting control regions of these two loci is specific as we found that the level of CpG methylation in bulk DNA, within the major and minor satellite DNA sequences and within endogenous C type retrovirus repeats, is not altered in the triple-H1 null ES cells. CpG methylation levels also were not altered in the promoter regions of the *α-actin* and the *Myl-c* genes, whose expression was not affected by H1 depletion. We suggest that the effect of H1 on DNA methylation in the two imprinting control regions is direct because H1 is indeed reduced by about one-half in these regions in the triple-H1 null ES cells (Figure S1 and data not shown). These results point to a previously unrecognized contribution of H1 to the control of gene expression in mammalian cells, namely through an effect on DNA methylation. In contrast, elimination of an H1-like gene in the filamentous fungus *Ascobolus immerses* was reported to have no effect on methylation-associated gene silencing, although it did lead to global hypermethylation (Barra et al., 2000), an effect we did not observe in mammalian cells. Recently, downregulation of H1 levels in *Arabidopsis thaliana* was reported to lead to both minor increases and decreases in the methylation patterns of certain repetitive and single-copy DNA sequences (Wierzbicki and Jerzmanowski, 2005). Therefore, H1 may play a role in regulating specific patterns of DNA methylation in both plants and animals.

Although changes in DNA methylation patterns at specific loci likely account for a substantial number of the gene-expression changes we observed in H1-depleted cells, it seems likely that other mechanisms are also involved. For example, our finding that 2 of the 19 genes that were upregulated encode H1 linker histones themselves suggests the existence of a feedback mechanism within the H1 gene family. The development of a cell-culture system in which highly specific changes in gene expression occur in response to H1 levels should allow a deeper understanding of the mechanisms by which linker histones participate in control of gene expression and possibly other aspects of chromatin regulation. The reintroduction of H1 genes into these cells also should make possible studies of linker-histone structure-function relationships in gene regulation.

EXPERIMENTAL PROCEDURES

Preparation and Analysis of ES Cell Nuclei and Histones

Cultured ES cells were trypsinized, washed once with PBS, resuspended in 0.5% NP-40 in RSB (10 mM NaCl, 3 mM $MgCl_2$, 10 mM Tris-HCl [pH 7.5]) with 1 mM phenylmethylsulfonyl fluoride (PMSF) at 4ºC, and homogenized by 10–15 strokes of pestle A in a Dounce homogenizer over a 20 min period. Released nuclei were centrifuged for 6 min at 1000 × g, and the nuclear pellets were resuspended in RSB containing 0.5 mM PMSF. Immunofluorescence microscopy and semiquantitative Western blotting of ES cells, nuclei, and nuclear proteins were carried out as described (Grigoryev et al., 2004). Histone proteins from ES cells were prepared by extraction of chromatin with 0.2N sulfuric acid as described previously (Fan et al., 2003).

Chromatin

For NRL analysis, nuclei were digested with 7–9 units of micrococcal nuclease (MNase) (Boehringer Mannheim) per 100 μg DNA for 5 min at 37ºC in RSB containing 1 mM $CaCl_2$ or with 15–30 units of enzyme per 100 μg of DNA for 5 min at 15ºC. For polynucleosomes, 2–3 units enzyme was used for 5 min at 15ºC. Reactions were terminated by adding 5 mM Na-EDTA. Nuclei were pelleted and resuspended in TE (pH 7.5). DNA electrophoresis was carried out as described previously (Fan et al., 2003). Psi-Plot (Poly Software International) was used for data analysis and graphing. For NRL analysis of specific gene loci, DNA fragments were transferred after electrophoresis to charged nylon membranes (GeneScreen Plus, PerkinElmer) by standard capillary blot conditions, and Southern blot analyses were carried out as described (Feinberg and Vogelstein, 1983). The *ADA* probe was a 820 bp HindIII/PstI fragment from middle of the gene. The *H19/Igf2* ICR-adjacent probe was a 484 bp BtsI-SfcI fragment prepared from construct pH19ICR (AP003183 GenBank accession number, nucleotide numbers 1433–1917).

Polynucleosomes were fractionated on 12 ml linear sucrose gradients (5%–40% w/v) containing 10 mM Tris-HCl (pH 7.5), 1 mM EDTA, and 5 mM NaCl in a Beckman SW41 rotor at 4ºC for 12 hr at 35,000 rpm. Fractions with chromatin longer than ~15 nucleosomes were combined, dialyzed against 10 mM HEPES, 1 mM EDTA, 5mM NaCl and concentrated in 100,000 MW cutoff Centricon filter devices (Millipore Inc., Bedford, MA; 100,000 MWCO). Samples were fixed by dialysis in 0.1% glutaraldehyde, 10 mM HEPES, 1 mM EDTA, 5 mM NaCl for 4 hr and then overnight in buffer alone.

Samples were prepared for electron microscopy as described (Woodcock and Horowitz, 1998; Georgel et al., 2003) and examined in a Tecnai 12 electron microscope at 100 kV or 80 kV, and images were recorded on a Temscan 2K CCD camera (TVIPS GmBH, Germany).

Oligonucleotide Microarrays

Exponentially growing ES cells were harvested after subculturing for 2 days at passage 9. Total RNA was extracted from ES cells using Trizol (Invitrogen) according to the manufacturer's protocol. One hundred micrograms of total RNA was purified with the RNeasy Mini Kit (QIAGEN). Fifteen micrograms of purified total RNA was used to synthesize cDNA with a T7-$(dT)_{24}$ primer and the SuperScript double-stranded cDNA synthesis kit (Life Technologies). cRNA labeling, hybridization to murine U74Av2 oligonucleotide array (Affymetrix, CA), washing, and staining were performed as recommended by Affymetrix. Fluorescent intensities were measured with a laser confocal scanner (HP Agilent 2200 confocal scanner), and data were analyzed with Affymetrix Microarray Software Suite (v5.0). Duplicate array hybridizations were performed with cRNA from two triple-H1 null ES cell lines and a wild-type littermate cell line.

Bisulfite Modification, PCR Amplification, and Pyrosequencing Analysis

One microgram of purified genomic DNA was treated with the Bisulfite Conversion Kit (CpG Genome) according to the manufacturer's manual. PCR conditions were the same as reported previously (Warnecke et al., 1998). The PCR primers for pyrosequencing were designed using PSQ Assay design software (Biotage AB, Uppsala). One of the PCR primers was biotinylated, and the biotinylated strands were purified and sequenced using PSQ HS 96 (Biotage AB). The data were processed and analyzed with PSQ HS 96A software (Biotage AB). The primer sequences and chromosomal regions analyzed are listed in Table S1.

Supplemental Data

Supplemental Data include Supplemental Experimental Procedures, Supplemental References, four figures, and one table and can be found with this article online at http://www.cell.com/cgi/content/full/123/7/1199/DC1/.

ACKNOWLEDGMENTS

This work was supported by NIH grants CA79057 (A.I.S.), GM43786 (C.L.W.), and GM62857 (A.S.). The authors wish to thank the AECOM Microarray Facility, the AECOM Laboratory of Macromolecular Analysis, and Christina Lowes at the AECOM Pyrosequencing Facility. We thank Dr. En Li for generously providing the pMO probe and *Dnmt1*$^{-/-}$ ES cell DNA and Dr. Michael Bustin for the generous gift of the affinity-purified anti-H1 antiserum. We thank Yamini Dalal for contributions toward the NRL determinations at the *ADA* locus, and we also thank Xing Han for technical assistance and Kevin Choe for helpful discussion. We also gratefully acknowledge technical advice from Dr. Winfried Edelmann, Elena Avdievich, and Diana Lin on ES cell-line derivation.

Received: January 20, 2005
Revised: August 5, 2005
Accepted: October 6, 2005
Published: December 28, 2005

REFERENCES

Allan, J., Harborne, N., Rau, D.C., and Gould, H. (1982). Participation of core histone "tails" in the stabilization of the chromatin solenoid. J. Cell Biol. *93*, 285–297.

Barra, J.L., Rhounim, L., Rossignol, J.L., and Faugeron, G. (2000). Histone H1 is dispensable for methylation-associated gene silencing in Ascobolus immersus and essential for long life span. Mol. Cell. Biol. *20*, 61–69.

Bednar, J., Horowitz, R.A., Grigoryev, S.A., Carruthers, L.M., Hansen, J.C., Koster, A.J., and Woodcock, C.L. (1998). Nucleosomes, linker DNA, and linker histone form a unique structural motif that directs the higher-order folding and compaction of chromatin. Proc. Natl. Acad. Sci. USA *95*, 14173–14178.

Bell, A.C., and Felsenfeld, G. (2000). Methylation of a CTCF-dependent boundary controls imprinted expression of the Igf2 gene. Nature *405*, 482–485.

Berkowitz, E.M., and Riggs, E.A. (1981). Characterization of rat liver oligonucleosomes enriched in transcriptionally active genes: evidence for altered base composition and a shortened nucleosome repeat. Biochemistry *20*, 7284–7290.

Carruthers, L.M., Bednar, J., Woodcock, C.L., and Hansen, J.C. (1998). Linker histones stabilize the intrinsic salt-dependent folding of nucleosomal arrays: mechanistic ramifications for higher-order chromatin folding. Biochemistry *37*, 14776–14787.

Clark, D.J., and Kimura, T. (1990). Electrostatic mechanism of chromatin folding. J. Mol. Biol. *211*, 883–896.

Clark, S.J., Harrison, J., Paul, C.L., and Frommer, M. (1994). High sensitivity mapping of methylated cytosines. Nucleic Acids Res. *22*, 2990–2997.

Dasso, M., Dimitrov, S., and Wolffe, A.P. (1994). Nuclear assembly is independent of linker histones. Proc. Natl. Acad. Sci. USA *91*, 12477–12481.

Dean, W., Bowden, L., Aitchison, A., Klose, J., Moore, T., Meneses, J.J., Reik, W., and Feil, R. (1998). Altered imprinted gene methylation and expression in completely ES cell-derived mouse fetuses: association with aberrant phenotypes. Development *125*, 2273–2282.

Dorigo, B., Schalch, T., Bystricky, K., and Richmond, T.J. (2003). Chromatin fiber folding: requirement for the histone H4 N-terminal tail. J. Mol. Biol. *327*, 85–96.

Fan, Y., Sirotkin, A., Russell, R.G., Ayala, J., and Skoultchi, A.I. (2001). Individual somatic H1 subtypes are dispensable for mouse development even in mice lacking the H1(0) replacement subtype. Mol. Cell. Biol. *21*, 7933–7943.

Fan, Y., Nikitina, T., Morin-Kensicki, E.M., Zhao, J., Magnuson, T.R., Woodcock, C.L., and Skoultchi, A.I. (2003). H1 linker histones are essential for mouse development and affect nucleosome spacing in vivo. Mol. Cell. Biol. *23*, 4559–4572.

Feinberg, A.P., and Vogelstein, B. (1983). A technique for radiolabeling DNA restriction endonuclease fragments to high specific activity. Anal. Biochem. *132*, 6–13.

Fletcher, T.M., and Hansen, J.C. (1996). The nucleosomal array: structure/function relationships. Crit. Rev. Eukaryot. Gene Expr. *6*, 149–188.

Georgel, P.T., Horowitz-Scherer, R.A., Adkins, N., Woodcock, C.L., Wade, P.A., and Hansen, J.C. (2003). Chromatin compaction by human MeCP2. Assembly of novel secondary chromatin structures in the absence of DNA methylation. J. Biol. Chem. *278*, 32181–32188.

Grigoryev, S.A., Nikitina, T., Pehrson, J.R., Singh, P.B., and Woodcock, C.L. (2004). Dynamic relocation of epigenetic chromatin markers reveals an active role of constitutive heterochromatin in the transition from proliferation to quiescence. J. Cell Sci. *117*, 6153–6162.

Hark, A.T., Schoenherr, C.J., Katz, D.J., Ingram, R.S., Levorse, J.M., and Tilghman, S.M. (2000). CTCF mediates methylation-sensitive enhancer-blocking activity at the H19/Igf2 locus. Nature *405*, 486–489.

Harvey, A.C., and Downs, J.A. (2004). What functions do linker histones provide? Mol. Microbiol. *53*, 771–775.

Hastie, N.D. (1989). Highly repeated DNA families in the genome of Mus musculus. In Genetic Variants and Strains of the Laboratory Mouse, Second Edition, M.F. Lyon and A.G. Searle, eds. (Oxford: Oxford University Press).

Hellauer, K., Sirard, E., and Turcotte, B. (2001). Decreased expression of specific genes in yeast cells lacking histone H1. J. Biol. Chem. *276*, 13587–13592.

Jackson-Grusby, L., Beard, C., Possemato, R., Tudor, M., Fambrough, D., Csankovszki, G., Dausman, J., Lee, P., Wilson, C., Lander, E., and Jaenisch, R. (2001). Loss of genomic methylation causes p53-dependent apoptosis and epigenetic deregulation. Nat. Genet. *27*, 31–39.

Kalitis, P., and Choo, K.H.A. (1989). Centromere DNA of higher eukaryotes. In The Centromere, K.H.A. Choo, ed. (New York: Oxford University Press).

Laybourn, P.J., and Kadonaga, J.T. (1991). Role of nucleosomal cores and histone H1 in regulation of transcription by RNA polymerase II. Science *254*, 238–245.

Lehnertz, B., Ueda, Y., Derijck, A.A., Braunschweig, U., Perez-Burgos, L., Kubicek, S., Chen, T., Li, E., Jenuwein, T., and Peters, A.H. (2003). Suv39h-mediated histone H3 lysine 9 methylation directs DNA methylation to major satellite repeats at pericentric heterochromatin. Curr. Biol. *13*, 1192–1200.

Li, E., Bestor, T.H., and Jaenisch, R. (1992). Targeted mutation of the DNA methyltransferase gene results in embryonic lethality. Cell *69*, 915–926.

Li, E., Beard, C., and Jaenisch, R. (1993). Role for DNA methylation in genomic imprinting. Nature *366*, 362–365.

Lin, S.P., Youngson, N., Takada, S., Seitz, H., Reik, W., Paulsen, M., Cavaille, J., and Ferguson-Smith, A.C. (2003). Asymmetric regulation of imprinting on the maternal and paternal chromosomes at the Dlk1-Gtl2 imprinted cluster on mouse chromosome 12. Nat. Genet. *35*, 97–102.

Maresca, T.J., Freedman, B.S., and Heald, R. (2005). Histone H1 is essential for mitotic chromosome architecture and segregation in Xenopus laevis egg extracts. J. Cell Biol. *169*, 859–869.

Misteli, T., Gunjan, A., Hock, R., Bustin, M., and Brown, D.T. (2000). Dynamic binding of histone H1 to chromatin in living cells. Nature *408*, 877–881.

Oswald, J., Engemann, S., Lane, N., Mayer, W., Olek, A., Fundele, R., Dean, W., Reik, W., and Walter, J. (2000). Active demethylation of the paternal genome in the mouse zygote. Curr. Biol. *10*, 475–478.

Patterton, H.G., Landel, C.C., Landsman, D., Peterson, C.L., and Simpson, R.T. (1998). The biochemical and phenotypic characterization of Hho1p, the putative linker histone H1 of Saccharomyces cerevisiae. J. Biol. Chem. *273*, 7268–7276.

Pennings, S., Meersseman, G., and Bradbury, E.M. (1994). Linker histones H1 and H5 prevent the mobility of positioned nucleosomes. Proc. Natl. Acad. Sci. USA *91*, 10275–10279.

Poirier, F., Chan, C.T., Timmons, P.M., Robertson, E.J., Evans, M.J., and Rigby, P.W. (1991). The murine H19 gene is activated during embryonic stem cell differentiation in vitro and at the time of implantation in the developing embryo. Development *113*, 1105–1114.

Ramon, A., Muro-Pastor, M.I., Scazzocchio, C., and Gonzalez, R. (2000). Deletion of the unique gene encoding a typical histone H1 has no apparent phenotype in Aspergillus nidulans. Mol. Microbiol. *35*, 223–233.

Reik, W., and Murrell, A. (2000). Genomic imprinting. Silence across the border. Nature *405*, 408–409.

Reik, W., and Walter, J. (2001). Genomic imprinting: parental influence on the genome. Nat. Rev. Genet. *2*, 21–32.

Ridsdale, J.A., Hendzel, M.J., Delcuve, G.P., and Davie, J.R. (1990). Histone acetylation alters the capacity of the H1 histones to condense transcriptionally active/competent chromatin. J. Biol. Chem. *265*, 5150–5156.

Schmidt, J.V., Matteson, P.G., Jones, B.K., Guan, X.J., and Tilghman, S.M. (2000). The Dlk1 and Gtl2 genes are linked and reciprocally imprinted. Genes Dev. *14*, 1997–2002.

Schwarz, P.M., and Hansen, J.C. (1994). Formation and stability of higher order chromatin structures. Contributions of the histone octamer. J. Biol. Chem. *269*, 16284–16289.

Shen, X., and Gorovsky, M.A. (1996). Linker histone H1 regulates specific gene expression but not global transcription in vivo. Cell *86*, 475–483.

Shen, X., Yu, L., Weir, J.W., and Gorovsky, M.A. (1995). Linker histones are not essential and affect chromatin condensation in vivo. Cell *82*, 47–56.

Shimamura, A., Sapp, M., Rodriguez-Campos, A., and Worcel, A. (1989). Histone H1 represses transcription from minichromosomes assembled in vitro. Mol. Cell. Biol. *9*, 5573–5584.

Sirotkin, A.M., Edelmann, W., Cheng, G., Klein-Szanto, A., Kucherlapati, R., and Skoultchi, A.I. (1995). Mice develop normally without the H1(0) linker histone. Proc. Natl. Acad. Sci. USA *92*, 6434–6438.

Sun, F.L., Cuaycong, M.H., and Elgin, S.C. (2001). Long-range nucleosome ordering is associated with gene silencing in Drosophila melanogaster pericentric heterochromatin. Mol. Cell. Biol. *21*, 2867–2879.

Takada, S., Paulsen, M., Tevendale, M., Tsai, C.E., Kelsey, G., Cattanach, B.M., and Ferguson-Smith, A.C. (2002). Epigenetic analysis of the Dlk1-Gtl2 imprinted domain on mouse chromosome 12: implications for imprinting control from comparison with Igf2–H19. Hum. Mol. Genet. *11*, 77–86.

Thoma, F., Koller, T., and Klug, A. (1979). Involvement of histone H1 in the organization of the nucleosome and of the salt-dependent superstructures of chromatin. J. Cell Biol. *83*, 403–427.

Thomas, J.O. (1999). Histone H1: location and role. Curr. Opin. Cell Biol. *11*, 312–317.

Tucker, K.L., Beard, C., Dausmann, J., Jackson-Grusby, L., Laird, P.W., Lei, H., Li, E., and Jaenisch, R. (1996). Germ-line passage is required for establishment of methylation and expression patterns of imprinted but not of nonimprinted genes. Genes Dev. *10*, 1008–1020.

Ushinsky, S.C., Bussey, H., Ahmed, A.A., Wang, Y., Friesen, J., Williams, B.A., and Storms, R.K. (1997). Histone H1 in Saccharomyces cerevisiae. Yeast *13*, 151–161.

van Holde, K.E. (1989). Chromatin (New York: Springer-Verlag).

Verona, R.I., Mann, M.R., and Bartolomei, M.S. (2003). Genomic imprinting: intricacies of epigenetic regulation in clusters. Annu. Rev. Cell Dev. Biol. *19*, 237–259.

Vignali, M., and Workman, J.L. (1998). Location and function of linker histones. Nat. Struct. Biol. *5*, 1025–1028.

Warnecke, P.M., Biniszkiewicz, D., Jaenisch, R., Frommer, M., and Clark, S.J. (1998). Sequence-specific methylation of the mouse H19 gene in embryonic cells deficient in the Dnmt-1 gene. Dev. Genet. *22*, 111–121.

Wierzbicki, A.T., and Jerzmanowski, A. (2005). Suppression of histone H1 genes in Arabidopsis results in heritable developmental defects and stochastic changes in DNA methylation. Genetics *169*, 997–1008. Published online October 16, 2004. 10.1534/genetics.104.031997.

Williams, S.P., Athey, B.D., Muglia, L.J., Schappe, R.S., Gough, A.H., and Langmore, J.P. (1986). Chromatin fibers are left-handed double helices with diameter and mass per unit length that depend on linker length. Biophys. J. *49*, 233–248.

Wolffe, A.P. (1998). Chromatin: Structure and Function (San Diego, CA: Academic Press).

Woodcock, C.L., and Horowitz, R.A. (1998). Electron microscopic imaging of chromatin with nucleosome resolution. Methods Cell Biol. *53*, 167–186.

Woodcock, C.L., Woodcock, H., and Horowitz, R.A. (1991). Ultrastructure of chromatin. I. Negative staining of isolated fibers. J. Cell Sci. *99*, 99–106.

Woodcock, C.L., Skoultchi, A.I., and Fan, Y. (2006). Role of linker histone in chromatin structure and function: H1 stoichiometry and nucleosome repeat length. Chromosome Res., in press.

Zlatanova, J., and Doenecke, D. (1994). Histone H1 zero: a major player in cell differentiation? FASEB J. *8*, 1260–1268.

Zlatanova, J., and Van Holde, K. (1992). Histone H1 and transcription: still an enigma? J. Cell Sci. *103*, 889–895.

Accession Numbers

Microarray data have been submitted to the Gene Expression Omnibus (GEO) under accession number GSE3714.